Journal of Autoimmunity 103 (2019) 102284

Contents lists available at ScienceDirect

Journal of Autoimmunity

journal homepage: www.elsevier.com/locate/jautimm

Impact of anti-CASPR2 autoantibodies from patients with autoimmune encephalitis on CASPR2/TAG-1 interaction and Kv1 expression

Margaux Saint-Martin[a,b,c,1], Alanah Pieters[a,b,c,1], Benoît Déchelotte[a,b,c], Céline Malleval[a,b,c], Delphine Pinatel[a,b,c], Olivier Pascual[a,b,c], Domna Karagogeos[e], Jérôme Honnorat[a,b,c,d], Véronique Pellier-Monnin[a,b,c], Nelly Noraz[a,b,c,*]

[a] INSERM U1217, Institut NeuroMyoGène, Lyon, F-69000, France
[b] CNRS UMR5310, Institut NeuroMyoGène, Lyon, F-69000, France
[c] University Claude Bernard Lyon 1, Lyon, F-69000, France
[d] Hospices Civils de Lyon, Lyon, F-69000, France
[e] University of Crete Medical School and IMBB-FORTH, Heraklion, Crete GR, 70013, Greece

ARTICLE INFO

Keywords:
CASPR2
TAG-1
Kv1
Autoimmune encephalitis
Autoantibody
Domains of interaction

ABSTRACT

Autoantibodies against CASPR2 (contactin-associated protein-like 2) have been linked to autoimmune limbic encephalitis that manifests with memory disorders and temporal lobe seizures. According to the growing number of data supporting a role for CASPR2 in neuronal excitability, CASPR2 forms a molecular complex with transient axonal glycoprotein-1 (TAG-1) and shaker-type voltage-gated potassium channels (Kv1.1 and Kv1.2) in compartments critical for neuronal activity and is required for Kv1 proper positioning. Whereas the perturbation of these functions could explain the symptoms observed in patients, the pathogenic role of anti-CASPR2 antibodies has been poorly studied. In the present study, we find that patient autoantibodies alter Caspr2 distribution at the cell membrane promoting cluster formation. We confirm in a HEK cellular model that the anti-CASPR2 antibodies impede CASPR2/TAG-1 interaction and we identify the domains of CASPR2 and TAG-1 taking part in this interaction. Moreover, introduction of CASPR2 into HEK cells induces a marked increase of the level of Kv1.2 surface expression and in cultures of hippocampal neurons Caspr2-positive inhibitory neurons appear to specifically express high levels of Kv1.2. Importantly, in both cellular models, anti-CASPR2 patient autoAb increase Kv1.2 expression. These results provide new insights into the pathogenic role of autoAb in the disease.

1. Introduction

Contactin-associated protein-like 2 (CASPR2) is a neuronal cell adhesion protein of the neurexin family expressed in the central and peripheral nervous system [1]. Autoantibodies (autoAb) against CASPR2 have been linked to acquired neuromyotonia (NMT) a peripheral nerve hyperexcitability syndrome [2], Morvan's syndrome (MoS), which combines NMT and encephalopathy [3] and autoimmune encephalitis (AE), a CNS-specific syndrome [4,5]. The presence of anti-CASPR2 Ab not only in serum but also in cerebrospinal fluid of AE patients was associated with rather homogeneous clinical features. They are men around 60 years of age with prevalent symptoms of limbic dysfunction, including memory disorders, temporal lobe seizures, and frontal lobe impairment [6,7]. CASPR2 autoAb were initially identified as Ab recognizing voltage-gated potassium channel (VGKC) [2]. However, it has become apparent that they principally target LGI1 or CASPR2. All these proteins belong to a complex referred as VGKC complex [8,9].

CASPR2 is a rather compact transmembrane protein with a C-terminal intracellular region that contains a 4.1B-binding motif and a type II PDZ-binding motif allowing, respectively, its interaction with cytoskeleton-associated proteins and scaffolding proteins. The extracellular part is composed of an N-terminal discoidin-like domain, four laminin G-like domains, two epidermal growth factor-like domains and a fibrinogen-like domain [10]. Anti-CASPR2 autoAb recognize multiple domains of the protein. Interestingly, all patients present autoAb directed against the discoidin and laminin G1 N-terminal domains and some, recognize only those two domains [6,7,11,12], suggesting that

* Corresponding author. INSERM U1217, CNRS UMR5310, Institut NeuroMyoGène (INMG), équipe SynatAc, Faculté de Médecine, 8 avenue Rockefeller, F-69008, Lyon, France.
E-mail address: nelly.noraz@inserm.fr (N. Noraz).
[1] Margaux Saint-Martin and Alanah Pieters have equally contributed to this work.

https://doi.org/10.1016/j.jaut.2019.05.012
Received 13 February 2019; Received in revised form 8 May 2019; Accepted 14 May 2019
Available online 06 June 2019
0896-8411/

Table 1
Primary and secondary antibodies. IF: Immunofluorescence; WB: Western blot; IP: Immunoprecipitation.

Antibodies	Species	Reference	Dilution
Anti-TAG-1 intra	rabbit	Millipore ABN1379	1/5000 (WB)
Anti-CASPR2 intra	rabbit	Abcam ab33994	1/5000 (WB)
Anti-CASPR2 intra	rabbit	Genscript A01426	1 µg (IP)
Anti-GFP	rabbit	ThermoFisher A-11122	1/5000 (WB), 1/1000 (IF)
Anti-HA	mouse	Sigma-Aldrich H3663	1/5000 (WB) 1/1000 (IF)
Anti-myc	mouse	Abcam ab9106	1 µg (IP)
Anti-Kv1.2 intra	mouse	NeuroMab K14/16	1/5000 (WB), 1/100 (IF)
Anti-Kv1.2 extra	rabbit	Alomone APC 162	1/100 (IF)
Anti-GAD65	mouse	Milipore MAB351	1/400 (IF)
Alexa 647 anti-rabbit	goat	Molecular Probes A21244	1/2000 (IF)
Alexa 405 anti-mouse	goat	Abcam ab175660	1/2000 (IF)
Alexa 555 anti-mouse IgG2b	goat	Molecular Probes A21147	1/1000 (IF)
Alexa 647 anti-mouse IgG2a	goat	Molecular Probes A21241	1/1000 (IF)
Alexa 488 anti-human	goat	Molecular Probes A11013	1/1000 (IF)
Alexa 488 anti-rabbit	goat	Molecular Probes A11034	1/1000 (IF)

autoAb binding to the discoidin and laminin G1 domains is involved in the development of the disease. Besides, anti-CASPR2 autoAb are mainly IgG4 [6,7], a subclass that binds weakly to Fc-γ receptors and do not activate complement. IgG4 could be considered as blocking Ab (i.e. Ab binding to its antigenic target disrupts its function).

CASPR2 forms a molecular complex with shaker-type voltage-gated potassium channels (Kv1.1 and Kv1.2) and transient axonal glycoprotein-1 (TAG-1), a glycosyl-phosphatidylinositol (GPI)-anchored adhesion molecule of the Ig superfamily also referred as Axonin-1 or Contactin-2 [13–16]. Proteins forming this complex were found co-enriched in compartments critical for neuronal activity including the axon initial segment (AIS) [17] and the juxtaparanodal region (JXP) of node of Ranvier (NOR) on myelinated axons [13,15]. Importantly, in CASPR2 KO mice, Kv1 and TAG-1 were no longer enriched at the JXP [13,18] and in the same way, in TAG-1 KO mice, Kv1 and CASPR2 were both mislocalized [15]. These data put into light the co-requirement of CASPR2 and TAG-1 for Kv1 proper positioning. In line with these findings and with the key function of Kv1 in controlling action potential propagation, CASPR2 has been involved in the regulation of intrinsic neuronal excitability [18,19]. In regards with anti-CASPR2 autoAb, some data support these findings. For instance, anti-CASPR2 autoAb impede CASPR2/TAG-1 interaction in a solid-phase binding assay [20]. Furthermore, CASPR2 autoAb enhance the excitability of DRG (dorsal root ganglion) neurons in a cell-autonomous fashion through regulation of Kv1 channel expression [19]. In the present study, experiments were conducted to bring further evidence of a pathogenic role of anti-CASPR2 autoAb in the disease.

2. Materials and methods

2.1. Patient sera and IgG purification

Sera from four patients with AE were obtained from the Centre National de Référence pour les Syndromes Neurologiques Paranéoplasiques in Lyon, France. All patients displayed temporal lobe seizures and memory disorders and were tested positive for anti-CASPR2 autoAb [6,21]. Informed consent was obtained for every patient and the present study was granted by the institutional review board of the Hospices Civils de Lyon (Comité de Protection des Personnes SUD-EST IV). We also used three control sera collected from healthy blood donors at Etablissement Français du Sang. The titer of anti-CASPR2 autoAb in the sera used in this study was previously determined using an HEK cell-based assay [6,21]. Importantly, serum antibody titers (last dilution of serum giving a positive signal) were high around 1:10.000 and equivalent among patients. To purify IgG, sera were incubated with protein-A Sepharose 4 Fast Flow™ beads (SIGMA) 2h at room temperature (RT) on rotation, transferred to columns and washed 3 times with PBS. IgG were eluted in glycine buffer pH2.8, neutralized in Tris buffer pH8.8 and dialyzed overnight at 4 °C in PBS (Slide-A-lyser G2 Dialysis Cassettes 0.5–3 ml ThermoFisher). IgG concentration was then measured using micro BCA protein assay kit (ThermoFisher). Purified IgG were sterilized on 0.22 µm filters and kept at −80 °C. Patient (Pat) and control (Ctl) IgG were either used separately or as a pool (pPat: equimolar concentration of Pat 2, Pat 3 and Pat 4 purified IgG; pCtl: equimolar concentration of Ctl 1, Ctl 2 and Ctl 3 purified IgG).

2.2. Constructs

The CASPR2-GFP plasmid, the CASPR2-HA (Hemagglutinin tag) and derived deleted constructs, CASPR2 Δ1, CASPR2 Δ2, CASPR2 Δ3, and CASPR2 Δ4, kindly provided by C. Faivre-Sarrailh, as well as CASPR2-Discoidin (D) and CASPR2-LamininG1 (L1) constructs were previously described [12]. The CASPR2-EGF2-LamininеG4 (E2L4) construct was obtained using reverse PCR on full-length CASPR2-HA plasmid and In-Fusion kit (Clontech). PCR amplified products were verified by sequencing (Eurofins). The TAG-1-GFP plasmid, TAG-1-GFP ΔFn and TAG-1-GFP ΔIg constructs, kindly provided by D. Karagogeos, were previously described [22]. The TAG-1-GFP ΔIg5 construct was obtained using reverse PCR on TAG-1-GFP full-length plasmid and In-Fusion kit (Clontech). The surface expression of proteins derived from all the plasmids used in this study has been validated in HEK cells (Fig. S1).

2.3. Antibodies

The primary and secondary antibodies used in this study are described in Table 1.

2.4. Cell lines and transfection

HEK 293 T cells were purchased from ATCC and cells referred in this paper as HEK-Kv were kindly provided by A. Morielli. HEK-Kv are HEK 293 cells stably expressing m1 mAChR, Kv1.2 and its Kvβ2 subunit [23]. Cells were grown in DMEM (ThermoFisher) SVF 10%, P/S 1% and transfected using the lipofectamine LTX kit (Invitrogen).

2.5. Immunoprecipitation and Western Blot

For immunoprecipitation (IP) and Western Blot analysis, 24 h after transfection HEK cells were lysed 10 min at 4 °C in lysis buffer pH7.5 containing NaCl 150 mM, HEPES 50 mM, Triton 1%, octyl-β-glucoside 60 mM (ThermoFisher), protease (Roche) and phosphatase (0.1 mM NaF, 0.1 mM Na3VO4, 1 mM PMSF, 1 mM benzamidine) inhibitors. Lysates were centrifuged at 4 °C, 10min 12000g, supernatant was

collected and protein concentration was evaluated using the micro BCA protein assay kit (ThermoFisher). Immunoprecipitation was performed using 150 µg of protein lysate and 1 µg of indicated Ab. Tubes were placed at 4 °C with rotation overnight and then protein G agarose fast flow beads (Millipore) were added for 2h. Supernatant was discarded and beads were washed three times in 500 µl lysis buffer. Immunoprecipitated proteins were then eluted in Laemmli DTT buffer, 5 min at 95 °C. Proteins were separated onto Criterion XT Bis-Tris precast 10% gels (Bio-Rad) and transferred onto nitrocellulose membrane (GE Healthcare). Membranes were blotted with the indicated Abs and revealed using Substrat HRP Immobilon Western (Millipore). Reactive proteins were visualized using the Chemidoc MP Imaging System (Bio-Rad). Band intensities were quantified using ImageJ and the ratio of protein co-immunoprecipitated/protein immunoprecipitated was calculated. In order to normalize for inter-experiment variations, ratios obtained for each condition were summed and results were expressed as a fraction of the summed ratios.

For surface immunoprecipitation transfected HEK cells were incubated with control or patient purified IgG (5 µg/mL) for 24 h at 37 °C. After one wash in PBS, cells were incubated with an anti-HA Ab or control anti-myc Ab (2 µg/mL) for 1h at room temperature, washed twice in PBS and lysed. Protein lysates were then processed as described above.

For the Biotinylation experiments hippocampal neurons (21 DIV) were treated for 24 h with pooled patient or control IgG and cell surface proteins were biotinylated using the Pierce Cell Surface Protein Isolation Kit (ThermoFisher) following manufacturer's instructions. The obtained total and surface fractions were denaturated for 5 min at 95 °C in Laemmli DTT and separated onto 4–15% Criterion TGX Stain-Free Precast Gels (Bio-Rad). Loaded proteins were quantified after transfer to nitrocellulose membrane using the Chemidoc MP Imaging System. Membranes were blotted with anti-CASPR2 Ab (ab33994). Reactive proteins were visualized with SuperSignal West Pico Chemiluminiscent Substrate (ThermoFisher, 34580) using the Chemidoc MP Imaging System. Band intensities were measured using Image Lab (version 5.2.1, Bio-Rad) and for each sample the ratio of Caspr2 to total loaded protein was calculated.

2.6. Flow cytometry

HEK-Kv cells were used for flow cytometry analysis. Cells were incubated with either patient or healthy control purified IgG at a concentration of 16 µg/mL for 24 h at 37 °C. HEK cells were washed with PBS one time and incubated with 154 mM sodium azide for 10 min at 37 °C, to limit endocytosis as previously described [24]. Cells were then washed with PBS and primary antibody was incubated for 1h at 4 °C in PBS 2% BSA. Cells were washed three times in PBS and secondary antibody was incubated for 30 min at 4 °C in PBS 2% BSA. After three washes in PBS, cells were then processed in the cytometer (three-laser FACS Canto II) and median of fluorescence intensity was measured for each parameter. In these experiments, Kv1.2 was labeled with anti-Kv1.2 Ab (APC 162) and Alexa647-conjugated secondary Ab; CASPR2 was labeled with anti-HA Ab and Alexa405-conjugated secondary Ab; TAG-1-GFP expression was directly measured. In order to normalize for inter-experiment variations, medians of fluorescence intensity obtained for each condition were summed and results were expressed as a fraction of the summed medians.

2.7. Primary hippocampal neuronal culture

Primary hippocampal neuron cultures were prepared from E18 Wistar rat embryos (Janvier Labs). Pregnant rats were deeply anesthetized by isoflurane (Ceva) inhalation and embryos were taken out by Caesarean section. Hippocampi were isolated in Hank's buffered salt solution (HBSS) (Gibco) and transferred for dissociation in HBSS supplemented with 10% (v/v) trypsin (Gibco) for 10 min at 37 °C. Hippocampi were then washed with 4% (w/v) bovine serum albumin (BSA) and triturated. Cells were plated onto poly-L-lysine (0.5 mg/mL) coated coverslips in Neurobasal medium (Gibco) supplemented with 2% (v/v) B27 (Gibco), 0.3% (v/v) L-glutamine (Invitrogen) and 1% (v/v) penicillin-streptomycin (invitrogen). Cells were cultured for 14 or 21 days at 37 °C in a humidified atmosphere containing 5% CO_2. Animal care and procedures were conducted according to the European Community Council Directive 2010/63/UE and the French Ethical Committee.

2.8. Immunocytofluorescence

For surface Caspr2 and total Kv1.2/GAD65 staining hippocampal neurons were treated at 20 DIV (days *in vitro*) with patient or control purified IgG at 16 µg/mL, for 24 h at 37 °C. At 21 DIV neurons were washed in Neurobasal and surface Caspr2 was stained using the pool of patient IgG (pPat) as primary Ab at 5 µg/mL, for 30 min at 37 °C. Neurons were then washed in Neurobasal, fixed in 4% (v/v) PFA for 10min, blocked with 3% (w/v) BSA in PBS for 30min and incubated for 30 min at RT with secondary Ab. After washing in PBS neurons were permeabilized for 30 min at RT with 3% (w/v) BSA in PBS 0.3% (v/v) Triton X-100 (PBS-T) and incubated for 1h at RT with anti-Kv1.2 (K14/16) and anti-GAD65 primary Ab. Neurons were then washed in PBS-T and incubated for 1h at RT with secondary Ab. After washing in PBS, nuclei were stained using 0.1 µg/mL Hoechst (ThermoFisher) for 5 min at RT.

For surface and total CASPR2-GFP staining, neurons were transfected at 18 DIV with CASPR2-GFP plasmid using the Lipofectamine LTX kit (Invitrogen) and treated at 20 DIV with pooled patient or control IgG at 16 µg/mL for 24 h at 37 °C. Neurons were washed in Neurobasal and surface CASPR2-GFP was stained with anti-GFP primary Ab for 30 min at 37 °C. Neurons were then washed in Neurobasal, fixed in 4% (v/v) PFA for 10min, blocked with 3% (w/v) BSA in PBS for 30min and incubated for 30 min at RT with alexa555 secondary Ab. After washing in PBS neurons were permeabilized for 30 min at RT with 3% (w/v) BSA in PBS-T and incubated for 1h at RT with anti-GFP primary Ab. Neurons were then washed in PBS-T and incubated for 1h with alexa488 secondary Ab. After washing in PBS, nuclei were stained using 0.1 µg/mL Hoechst (ThermoFisher) for 5 min at RT.

For all experiments coverslips were mounted in FluorPreserve Reagent (Calbiochem) and stored at 4 °C until image acquisition.

2.9. Image acquisition and analysis

Images were acquired using Zeiss Axio Imager Z.I ApoTome microscope and for the quantitative analysis a fixed exposition time was applied to the different experimental conditions. To quantify surface Caspr2 signal intensities, images were analyzed using ICY Spotdetector Plugin (version 1.9.10.0, BioImage Analysis Unit Institut Pasteur). The mean intensity of the clusters/spots detected was multiplied by cluster area to get total signal intensity per cluster. Values were summed and divided by total surface occupied by clusters. Results were expressed as mean Caspr2 signal intensity.

To analyze surface CASPR2-GFP expression, a ROI corresponding to transfected neuron was defined based on the surface occupied by green signal (total CASPR2-GFP). Red signals (surface CASPR2-GFP) included in the ROI were then quantified using ICY Spotdetector and results depicted as cluster size, cluster intensity and cluster number per μm^2 of neuron.

To analyze Kv1.2 expression, ROIs with the same surface across different experimental conditions were defined along neurites based on the red signal (surface Caspr2). Green signal intensities (total Kv1.2) included in the ROI were then quantified using ICY and results depicted as intensity arbitrary units.

2.10. Statistical analysis

GraphPad Prism software was used for all statistical tests. Depending on the experimental setting, data were compared using a Mann-Whitney, a Kruskal-Wallis or a Wilcoxon signed-rank test. Data were represented as mean ± SD and significance was set for a p value ≤ 0.05.

3. Results

3.1. Patient anti-CASPR2 autoAb impede CASPR2/TAG-1 interaction

Using an acellular solid phase binding assay, it has been shown that CASPR2 and TAG-1 directly interact through their extracellular domains and that anti-CASPR2 patient sera inhibited this interaction [20]. Here, in a first set of experiments, we asked whether anti-CASPR2 autoAb from AE patients were able to perturb CASPR2/TAG-1 interaction in a cellular model. HEK cells co-transfected with CASPR2-HA and TAG-1-GFP were incubated for 24 h with healthy donor (Ctl) or patient (Pat) IgG purified from serum to avoid any side effects due to other serum proteins. Cells were then further incubated with an anti-HA Ab before lysis to specifically immunoprecipitate the fraction of CASPR2 present at the cell surface. The ratio of TAG-1 co-immunoprecipitated (co-IP) over CASPR2 immunoprecipitated (IP) was assessed. As shown in Fig. 1A, co-IP TAG-1 was observed in surface CASPR2 immunoprecipitates obtained from cells treated with Ctl or Pat IgG, but not in the control immunoprecipitates (Ctl IP) for which co-transfected HEK cells were incubated 24 h with PBS and incubated with an irrelevant control Ab before lysis. Compared with Ctl IgG the level of co-IP TAG-1 was diminished in Pat IgG treated cells (Ctl: 0.55 ± 0.09; Pat: 0.44 ± 0.09 $p < 0.01$). Notably, a 20% and 19% decrease of TAG1-binding was observed using patient 2 and patient 3 IgG respectively whereas decreased binding was rather low on cells incubated with patient 1 IgG (7% decrease) and not observed with patient 4 IgG (Fig. 1B).

3.2. The EGF2 and laminin G4 domains of CASPR2 are critical for TAG-1 interaction

To get a better understanding of the decreased CASPR2/TAG-1 binding observed in the presence of patient autoAb, we conducted experiments to determine which domain(s) of either protein was responsible for their interaction. Notably, both CASPR2/TAG-1 cis- and trans-interactions have been reported [13,15,25] and in CASPR2 and TAG-1 co-transfected HEK cells, both types of interactions are possible. We therefore first evaluated the contribution of CASPR2/TAG-1 trans-interactions in our model. To this end, HEK cells were either, co-transfected with plasmids coding for CASPR2-HA and TAG-1-GFP proteins (C2T1) allowing cis and trans associations or, cells were separately transfected with either one plasmids and subsequently put together (C2 + T1) allowing CASPR2/TAG-1 trans-associations only (Fig. 2A left panel). Cells were lysed and CASPR2 was immunoprecipitated using a commercial antibody directed against its intracellular domain (ab33994). As shown in Fig. 2A right panel, the level of TAG-1 co-IP

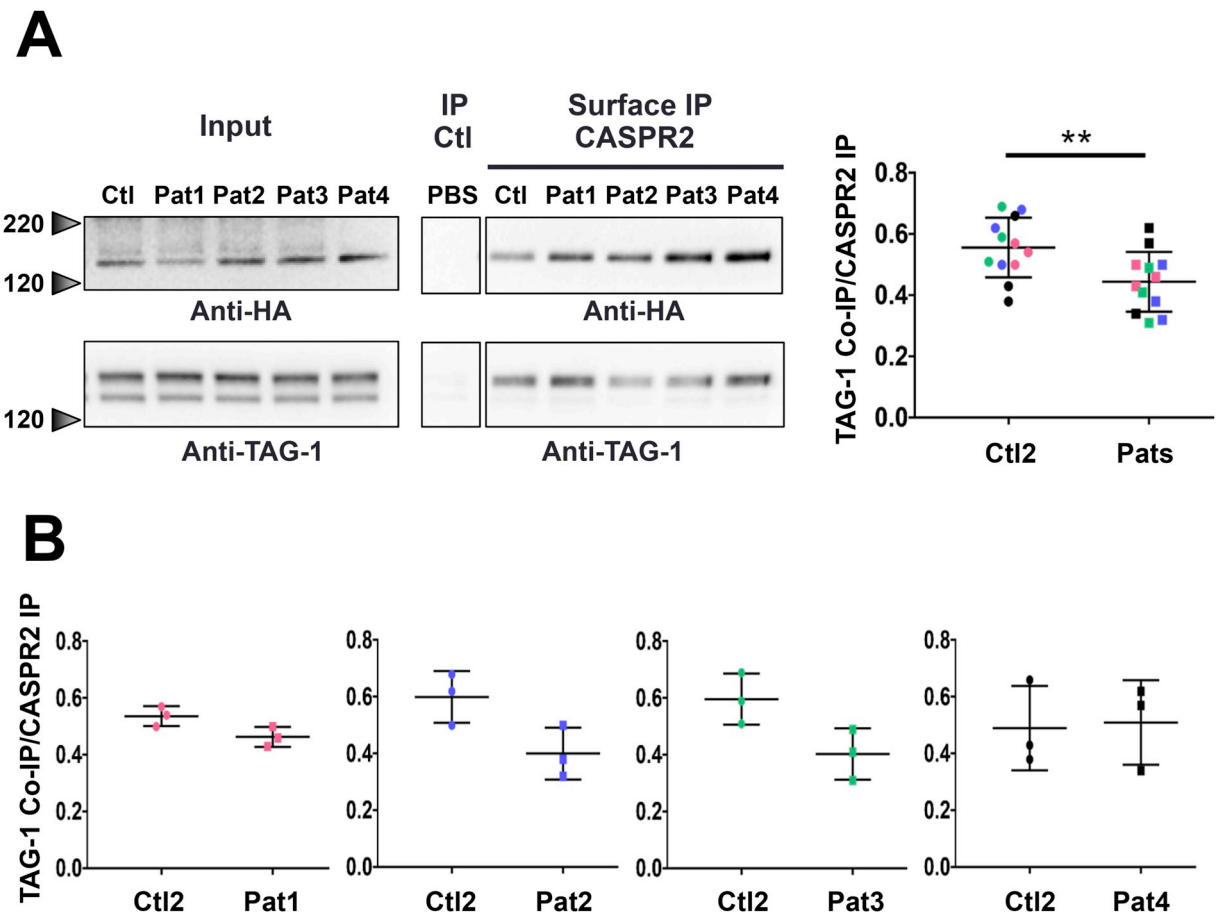

Fig. 1. Patient autoAb impede CASPR2/TAG-1 interaction A) HEK cells co-transfected with CASPR2-HA and TAG-1-GFP were incubated for 24 h with serum-purified control IgG (Ctl) or patient IgG (Pat). CASPR2 present at the cell surface was IP (surface IP) and the level of CASPR2 IP or TAG-1 co-IP, was analyzed by Western Blot. As control, co-transfected HEK cells were incubated with PBS and IP with a control Ab. The ratios of TAG-1 co-IP over CASPR2 IP signal intensities are depicted. Each color represents a different patient. n = 12 obtained from 3 independent cultures, **p < 0.01 Mann-Whitney test. **B)** Ratios of TAG-1 Co-IP over CASPR2 IP are represented separately for each patient.

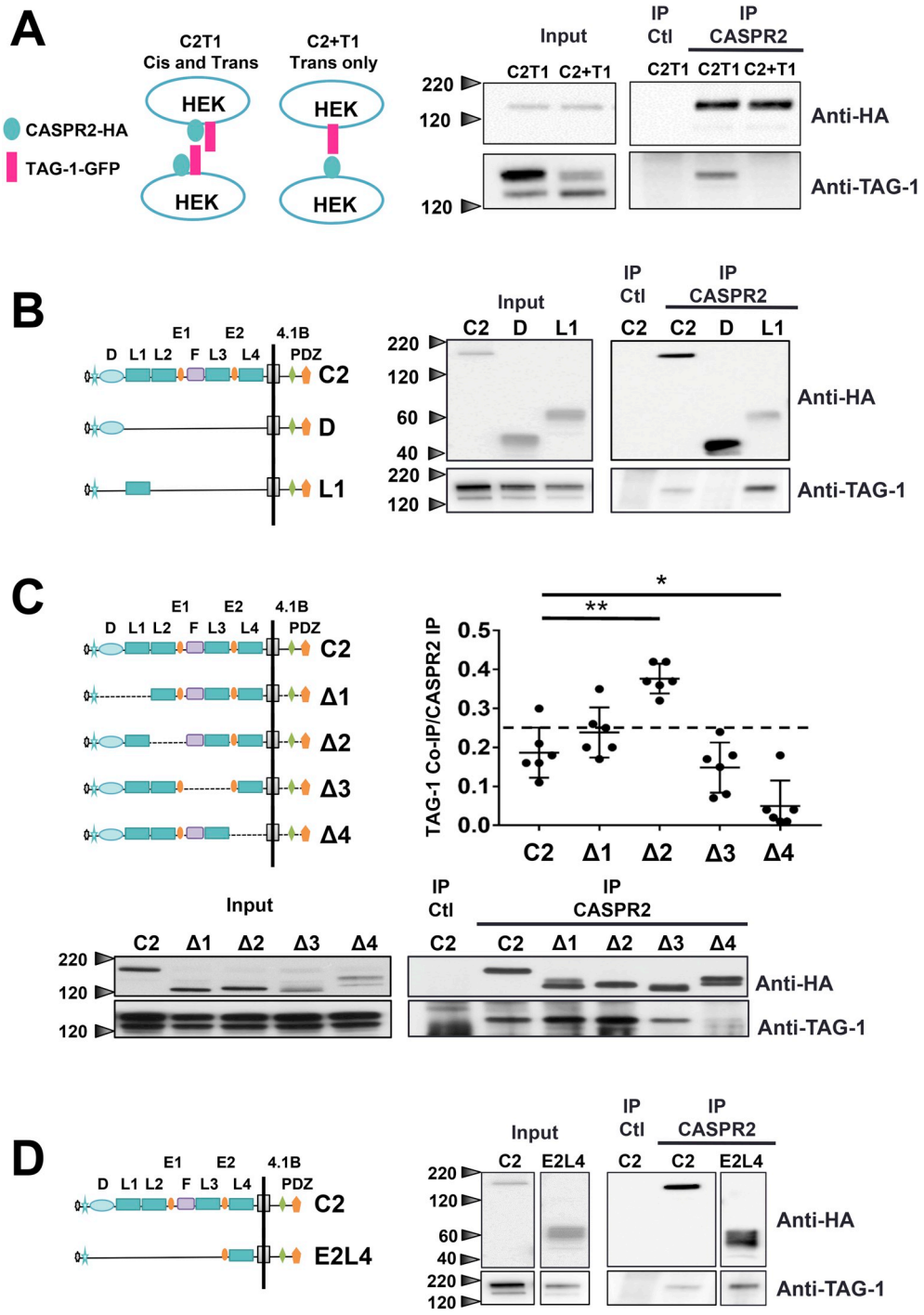

Fig. 2. The EGF2 and laminin G4 domains of CASPR2 are critical for TAG-1 interaction. A) HEK cells were co-transfected with CASPR2-HA and TAG-1-GFP (C2T1) or separately transfected with either one and subsequently put together (C2 + T1). CASPR2 was IP and the level of CASPR2 IP or TAG-1 co-IP was analyzed by Western Blot. n = 3. **B-D)** HEK cells were co-transfected with TAG-1-GFP and CASPR2-HA full-length (C2) or the indicated mutants. CASPR2 was IP and the level of CASPR2 IP and TAG-1 co-IP was analyzed by Western Blot. **(B)** CASPR2 discoidin (D) and laminin G1 (L1) mutants. n = 3. **(C)** CASPR2 Δ1 to Δ4 deletion mutants. The ratios of TAG-1 co-IP over CASPR2 IP signal intensities are depicted in a dot plot. n = 6, *p < 0.05, **p < 0.01 Mann-Whitney test. **(D)** CASPR2 EGF2-laminin G4 mutant (E2L4). n = 3. D: discoidin-like domain, L: laminin G-like domain, E: EGF-like domain, F: fibrinogen-like domain, 4.1B: 4.1B-binding motif, PDZ: PDZ-binding motifs.

was much higher in co-transfected cells (C2T1) than in cells separately transfected (C2 + T1) for which TAG-1 was barely detectable even at long exposure times. These data indicate that the majority of the TAG-1 co-IP with CASPR2 in co-transfected cells comes from cis-interaction between the two proteins.

Anti-CASPR2 autoAb from AE patients all recognize the N-terminal discoidin (D) and laminin G1 (L1) domains of CASPR2 and more importantly, 45% of patient autoAb recognize only these two domains [6], suggesting that they could be critical for CASPR2/TAG-1 interaction. To test this hypothesis, TAG-1 co-IP were repeated as described above in cells expressing the full-length (C2) or only the discoidin (D) or laminin G1 (L1) domains of CASPR2. No TAG-1 co-IP was detected in cells expressing the discoidin domain of CASPR2 (Fig. 2B). In contrast, the laminin G1 domain of CASPR2 was sufficient to co-IP TAG-1 (Fig. 2B). To further characterize the domains of CASPR2 involved in TAG-1 interaction, the same experiment was performed using deletion constructs covering the entire CASPR2 protein. CASPR2 was IP and co-IP TAG-1 was quantified (Fig. 2C). As previously shown [26], compared with CASPR2 full-length (C2), deletion of the laminin G2 and EGF1 domains of CASPR2 (Δ2) increased the quantity of TAG-1 co-IP (C2: 0.19 ± 0.06; Δ2: 0.38 ± 0.04 $p < 0.01$) (Fig. 2C). Although this result did not tell much about the TAG-1-binding propensity of the laminin G2 and EGF1 domains of CASPR2, it suggested that CASPR2/TAG-1 interaction is constrained by conformational hindrances. Equal levels of TAG-1 were co-IP in cells transfected with the CASPR2 construct lacking the discoidin and laminin G1 domains (Δ1) or the

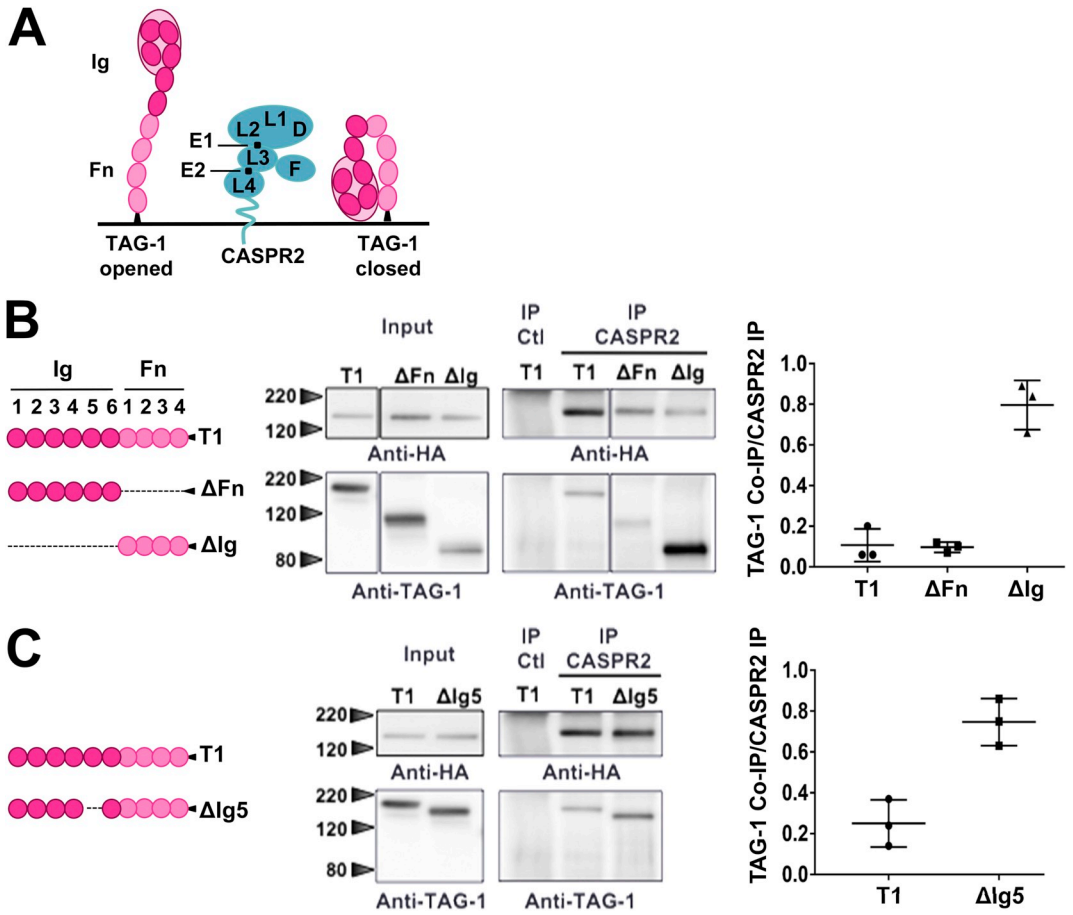

Fig. 3. Both the Ig and Fn domains of TAG-1 are involved in CASPR2/TAG-1 interaction. A) Models of CASPR2 and TAG-1 domain assignment in three dimensions. **B–C)** HEK cells were co-transfected with CASPR2-HA and TAG-1-GFP full-length (T1) or deletion mutants. (**B**) TAG-1 ΔFn and TAG-1 ΔIg. (**C**) TAG-1 ΔIg5. CASPR2 was IP and the level of CASPR2 IP and TAG-1 co-IP was analyzed by Western Blot. The ratios of TAG-1 co-IP over CASPR2 IP signal intensities are depicted in a dot plot. n = 3.

fibrinogen and laminin G3 domains (Δ3) (C2: 0.19 ± 0.06; Δ1: 0.24 ± 0.06; Δ3: 0.15 ± 0.06, $p > 0.05$) indicating that these domains are dispensable for CASPR2/TAG-1 interaction (Fig. 2C). In contrast, the Δ4 construct lacking the EGF2 and laminin G4 domains of CASPR2 led to a drastic decrease of CASPR2/TAG1 interaction (C2: 0.19 ± 0.06; Δ4: 0.05 ± 0.07 $p < 0.05$) (Fig. 2C) indicating that they are major domains of interaction. According to this, the construct expressing only the EGF2 and laminin G4 domains of CASPR2 (E2L4) was sufficient to co-IP TAG-1 (Fig. 2D).

To recapitulate, of the two discoidin and laminin G1 domains, only the laminin G1 domain is involved in CASPR2/TAG-1 interaction and the removal of these domains does not significantly hamper CASPR2/TAG-1 binding. On the contrary, the EGF2 and laminin G4 domains are critical for CASPR2/TAG-1 interaction.

3.3. Both the Ig and Fn domains of TAG-1 are involved in CASPR2/TAG-1 interaction

TAG-1 consists of 6 immunoglobulin (Ig) domains followed by 4 fibronectin domains (Fn) tethered to the cell surface by a GPI anchor (Fig. 3A). The fact that the EGF2-laminin G4 domains of CASPR2, the main interaction domains involved in CASPR2/TAG-1 interaction, are located near the membrane was difficult to conciliate with previous findings showing that CASPR2 interacts in cis with the Ig but not the Fn domains of TAG-1 [22]. Therefore, the ability of CASPR2 to interact with the Ig and Fn domains of TAG-1 was re-considered. Deletion of neither TAG-1 Fn1-4 domains (ΔFn) nor Ig1-6 domains (ΔIg) prevented CASPR2 binding to TAG-1 indicating that both are involved in CASPR2/TAG-1 interaction. Moreover, the removal of TAG-1 Ig domains increased CASPR2 binding suggesting that Ig domains placed constraints on CASPR2 accessibility to TAG-1 Fn domains (Fig. 3B). It has been proposed that TAG-1 could adopt various shapes ranging from a horseshoe-shape or closed conformation to an extended shape or opened conformation (Fig. 3A) [27]. One can therefore postulate that in the closed conformation the Fn domains could be masked by the Ig domains thus limiting their binding to CASPR2. Inversely, in the opened conformation accessibility of Fn domains to CASPR2 could be promoted. To test this hypothesis, we used the TAG-1 ΔIg5 mutant previously described to shift the conformation of the protein toward an extended shape favoring Fn domains exposure [28]. As shown in Fig. 3C, the level of TAG-1 co-IP was higher in cells transfected with TAG-1 ΔIg5 than the full-length construct.

Together, these results indicate that although both the Fn and Ig domains of TAG-1 are involved in CASPR2/TAG-1 interaction, in the TAG-1 back-folded conformation Ig domains could limit TAG-1 binding to CASPR2.

3.4. Patient autoAb do not alter CASPR2 surface expression but increase Kv1.2 surface expression

Based on findings suggesting that CASPR2 and TAG-1 affect intrinsic neuronal excitability by impacting Kv1 expression/distribution at the membrane [18,19,29], we wanted to test the hypothesis that patient anti-CASPR2 autoAb could alter Kv1.2 surface expression. As a preliminary experiment, we wished to determine whether CASPR2 or TAG-1 expression could impact Kv1.2 surface expression. To this end, we

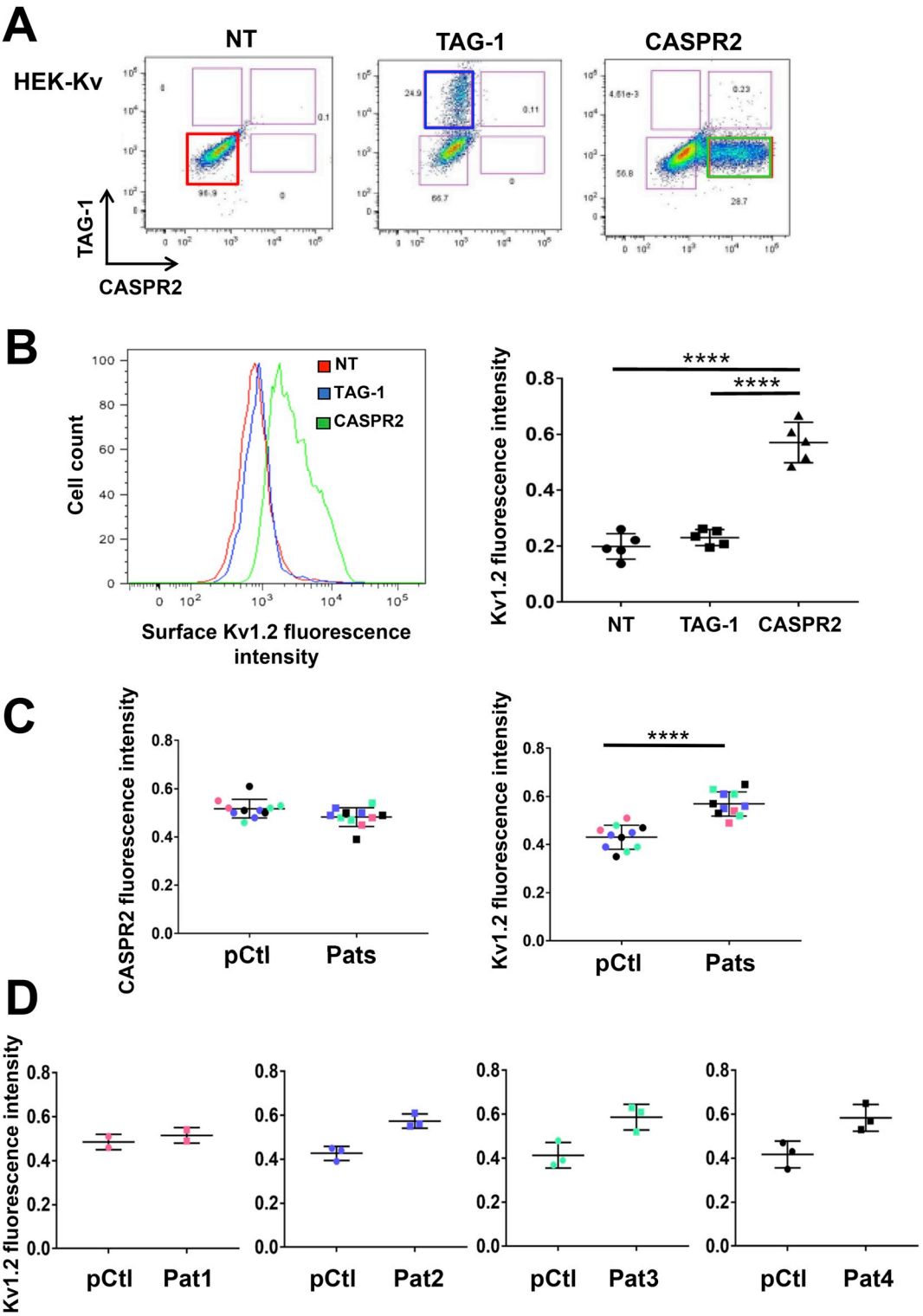

Fig. 4. Patient autoAb do not alter CASPR2 surface expression but increase Kv1.2 surface expression. HEK cells stably expressing Kv1.2 (HEK-Kv) were either non-transfected (NT) or transfected with CASPR2-HA or TAG-1-GFP. The level of Kv1.2 surface expression was quantified by flow cytometry. **A)** Dot plot representation of TAG-1 and CASPR2 fluorescence intensity in the whole population of cells. Non-transfected, TAG-1-positive and CASPR2-positive gated populations are shown in color boxes. **B)** Histogram representation of surface Kv1.2 fluorescence intensity measured in the gated populations shown in A). Results are depicted in a dot plot as mean Kv1.2 fluorescence intensity ratio. n = 5, $p < 0.0001$ Mann-Whitney test. **C)** HEK-Kv cells co-transfected with CASPR2-HA and TAG-1-GFP were incubated for 24 h with pooled control (pCtl) or Patient (Pats) IgG. CASPR2 and Kv1.2 surface fluorescence intensity was measured. Results are depicted as a fraction of the summed median fluorescence intensities. Each color represents a different patient. n = 11 obtained from 3 independent experiments, ****$p < 0.0001$ Mann-Whitney test. **D)** Surface Kv1.2 fluorescence intensity for each patient.

used HEK cells stably expressing Kv1.2 and its Kvβ2 subunit (HEK-Kv) [23]. HEK-Kv cells were transfected with CASPR2-HA or TAG-1-GFP and the level of Kv1.2 surface expression was quantified by flow cytometry (Fig. 4A). As depicted in Fig. 4B, the level of Kv1.2 in TAG-1-positive gated cells was not different from the control non-transfected cells (NT) (0.23 ± 0.03 versus 0.20 ± 0.05, $p > 0.05$). In contrast, Kv1.2 expression was markedly increased following CASPR2 transfection (CASPR2: 0.57 ± 0.07 versus NT: 0.20 ± 0.05, $p < 0.0001$).

Next, HEK-Kv co-transfected with CASPR2-HA and TAG-1-GFP were incubated for 24 h in the presence of Ctl lgG or Pat IgG and the level of CASPR2 and Kv1.2 surface expression was assessed (Fig. 4C). Whereas CASPR2 surface expression was not affected, (Ctl: 0.52 ± 0.02; Pat: 0.48 ± 0.02, $p > 0.05$), the level of Kv1.2 surface expression was significantly increased by patient IgG (Ctl: 0.44 ± 0.03; Pat: 0.56 ± 0.03, $p < 0.0001$). Patient 2, 3 and 4 increased Kv1.2 surface expression to a similar extent, 15.22%, 16.71%, and 16.52% respectively while Patient 1 only induced a 3.15% increase (Fig. 4D).

3.5. Patient autoAb alter CASPR2 surface distribution in hippocampal neurons

To study the impact of anti-CASPR2 autoAb in a more relevant cellular model, cultures of primary hippocampal neurons were treated at 20 DIV with patient IgG (Pat 2, Pat 3, Pat 4) or control IgG (Ctl 1, Ctl 2). Since no commercial Ab targeting the extracellular part of Caspr2 was available at that time, surface Caspr2 labeling was performed using a pool of patient IgG (pPat). In agreement with previous data [12], Caspr2 staining appeared as clusters of various sizes and intensities. Only a subpopulation representing approximately 20% of neurons expressed Caspr2. Moreover, Caspr2 was essentially localized along axons (Fig. 5A and data not shown).

Compared with Ctl IgG, a two-fold increase of Caspr2 surface intensity was observed upon incubation with the three patient IgG tested (Fig. 5A). To gain confidence in these results, the experiment was repeated using pooled patient (pPat) or control (pCtl) IgG and surface Caspr2 was assessed using a cell surface biotinylation assay (Fig. 5B). Notably, the level of Caspr2 in the biotinylated fraction of the proteins as well as the level of total Caspr2 was not different between the two conditions. Finally, to get a better idea of the impact of patient IgG on Caspr2 level of expression and distribution at the cell surface, hippocampal neurons were transfected with a plasmid coding for CASPR2-GFP and then treated with pooled patient IgG (pPat) or control IgG (pCtl). To analyze the fraction of CASPR2 present at the cell surface, live cells were labeled with an anti-GFP primary Ab and an anti-rabbit Alexa555-conjugated secondary Ab, therefore avoiding any interference between patient Ab used during the 24h incubation and Ab used for CASPR2 surface labeling. CASPR2 mean surface intensity per um2 of neuron was higher in cells incubated with Pat IgG than Ctl IgG (pPat: 11.62 ± 6.86; pCtl: 1.02 ± 0.81 $p < 0.0001$, data not shown). The size, intensity and number of CASPR2 clusters were then quantified for each condition and compared (Fig. 5C). Whereas patient IgG induced a two-fold increase in cluster intensity (pCtl: 16.43 ± 4.32; pPat: 32.60 ± 10.39 $p < 0.0001$), a slight increase in cluster size was observed (pCtl: 0.20 ± 0.02; pPat: 0.25 ± 0.05 $p < 0.0001$). In contrast, CASPR2 cluster number at the cell surface was markedly augmented (pCtl: 0.06 ± 0.04; pPat: 0.32 ± 0.09 $p < 0.0001$).

Taken together, these results showed that patient IgG did not induce Caspr2 internalization but altered its distribution at the cell membrane promoting Caspr2 cluster formation.

3.6. Patient autoAb increase Kv1.2 expression in hippocampal neurons

In line with the results we obtained on HEK cells, the impact of anti-CASPR2 patient autoAb on Kv1.2 expression was assessed in hippocampal neurons (21 DIV). Firstly, cells were stained for Kv1.2 surface expression but we were not able to observe any signal. Therefore, Caspr2 expression was assessed on live cells (surface) using the pool of patient IgG and Kv1.2 expression was assessed on permeabilized cells (total). As illustrated in Fig. 6A, fibers expressing high level of Kv1.2 could be clearly distinguished and strikingly an obvious co-labeling was observed with axons highly positive for Caspr2. Since in cultured hippocampal neurons Caspr2 is essentially expressed in inhibitory neurons [12], cells were stained for GAD65, a typical marker of inhibitory neurons (Fig. 6A). As expected the population of axons highly positive for Caspr2 was essentially GAD65-positive (98%) moreover, 90% of the Caspr2/GAD65-double positive axons also expressed high level of Kv1.2. Therefore, it appeared that Caspr2-positive inhibitory neurons also express high level of Kv1.2. Secondly, to determine whether anti-CASPR2 patient Ab modulate Kv1.2 expression, primary hippocampal neurons were treated at 20 DIV with the pool of patient or control IgG and stained for surface Caspr2 and total Kv1.2 (Fig. 6B). Compared with control IgG, treatment with patient IgG significantly increased Kv1.2 signal intensity (Ctl: 409.8 ± 83.2 versus Pat: 568.9 ± 193.6, $p < 0.01$).

4. Discussion

4.1. Anti-CASPR2 patient autoAb alter CASPR2 surface distribution

We show in this study that patient autoAb do not induce CASPR2 internalization using two cellular models, HEK cells and more importantly cultured primary hippocampal neurons. When tested on endogenous Caspr2, the level of Caspr2 at the cell surface remained essentially unchanged upon patient autoAb addition. However, in CASPR2 transfected neurons, patient IgG increased CASPR2 surface expression. Moreover, CASPR2 membrane distribution was altered with the formation of an elevated number of CASPR2 clusters. In view of these observations, it appears that the pathogenic effect of autoAb rely on CASPR2 redistribution at the cell membrane rather than internalization. These results are consistent with the fact that anti-CASPR2 patient autoAb are often IgG4 [6,7,12], a subclass presenting several unique biophysical properties. In particular, IgG4 can undergo half-molecule exchange rendering them bispecific and thereby functionally monovalent. This implies that IgG4 are unable to crosslink their targets which is often a prerequisite for the process of internalization [30].

4.2. Anti-CASPR2 patient autoAb impede CASPR2/TAG-1 interaction

It was suggested that patient autoAb could directly perturb CASPR2 function by preventing CASPR2/TAG-1 interaction. For instance, using an acellular solid phase binding assay, Patterson et al. [20] showed that patient Ab decrease CASPR2/TAG-1 binding by 30%–90% depending on the patient serum tested. In this paper, using purified serum IgG, we find that the decrease of CASPR2/TAG-1 binding upon anti-CASPR2 autoAb addition still occurs in a cellular environment, although to a lower extent (under 20% of decrease). Moreover, we identified regions taking part in CASPR2/TAG-1 cis-interactions, the Ig1-6 and Fn1-4 domains on TAG-1 side as well as the laminin G1 and the EGF2-laminin G4 domains on CASPR2 side. However, the removal of the laminin G1 domain of CASPR2 did not significantly hamper CASPR2/TAG-1 interaction, whereas removal of the EGF2-laminin G4 domains drastically impeded CASPR2/TAG-1 interaction, pointing the EGF2-laminin G4 domains as key domains of interaction. EGF-like domains consist of molecular hinges (small linear solenoid domain) permitting the lobes of the protein to flex with respect to each other [31,32]. In contrast, laminin G-like domains are large globular domains involved in interactions with other proteins (neuroligin, cerebellin, GABAa receptor) [33,34]. It is therefore likely that the laminin G4 domain of CASPR2, rather than the EGF2 domain, mediates CASPR2/TAG-1 interactions. Considering the molecular shape and dimension of these two molecules a model can be proposed for which the laminin G4 domain of CASPR2 interacts with the fibronectin domains of TAG-1 and the laminin G1

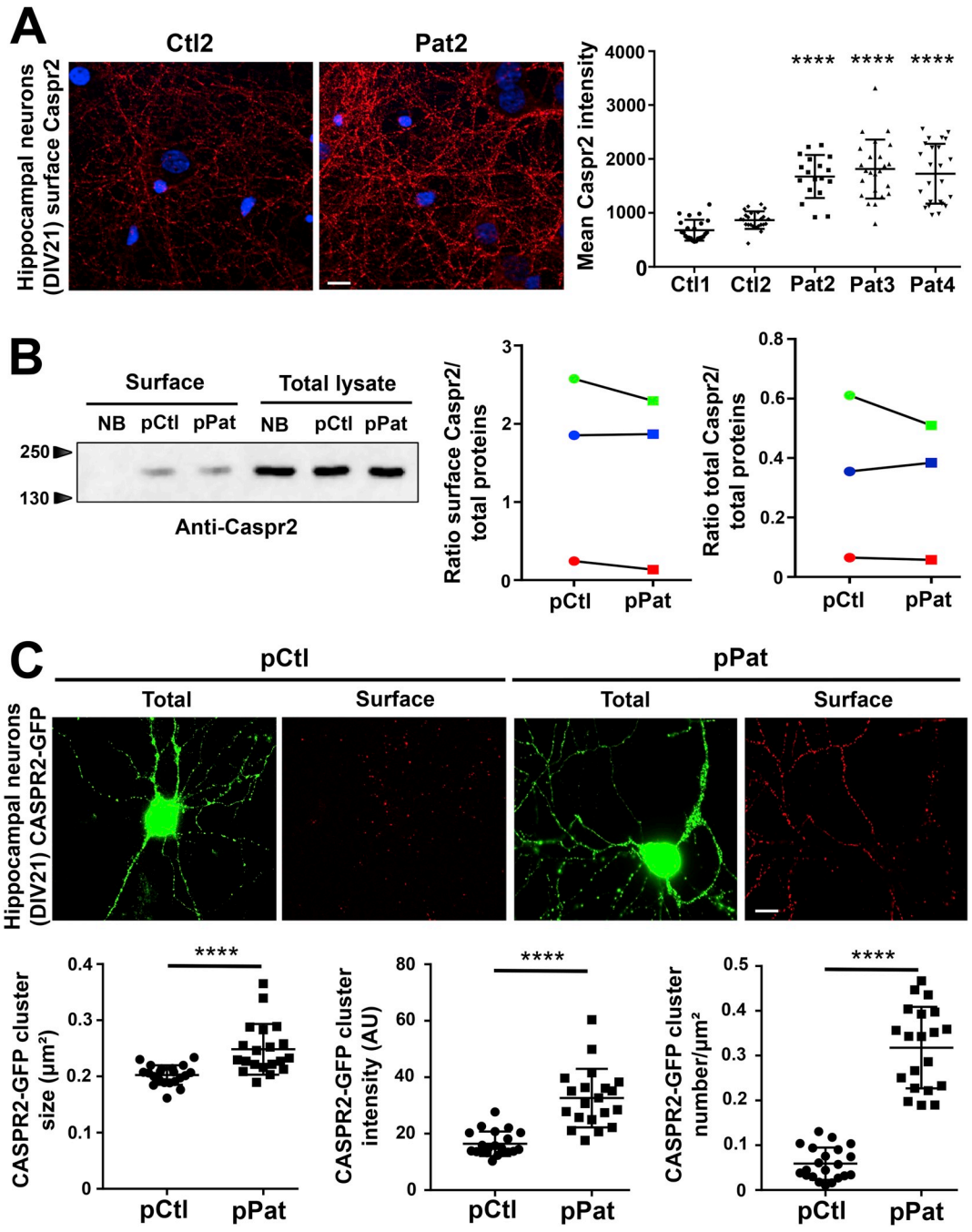

Fig. 5. Patient autoAb changed CASPR2 surface distribution in hippocampal neurons. A) hippocampal neurons (21 DIV) treated for 24h with control (Ctl) or patient (Pat) IgG were stained for surface Caspr2 and signal intensities were quantified. n = 17–24 image fields per condition, ****p < 0.0001 Kruskal-Wallis test. **B)** Hippocampal neurons (21 DIV) treated with pooled patient (pPat) or control (pCtl) IgG were subjected to cell surface biotinylation or left non-biotinylated as control (NB). Caspr2 surface and Caspr2 total proteins were quantified by Western-Blot and results expressed as ratios over total protein loaded. Each color represents a different experiment. n = 3, Wilcoxon signed-rank test. **C)** Hippocampal neurons (21 DIV) transfected with CASPR2-GFP were treated with pooled patient (pPat) or control (pCtl) IgG. The size, intensity and number of surface CASPR2-GFP clusters was analyzed on live cells using anti-GFP primary Ab/Alexa555 secondary Ab. Results are depicted as a dot plot. n = 21 neurons per condition obtained from 3 independent experiments, ****p < 0.0001 Mann-Whitney test. Scale bar 10 µm.

domain of CASPR2 interacts with the immunoglobulin domains of TAG-1 (Fig. 7A). Essentially obtained with deletion mutants, this model has nevertheless to be taken with caution since we find here that as depicted by others [32], CASPR2/TAG-1 interactions are constrained by conformational hindrances.

Regarding the impact of anti-CASPR2 autoAb on this model of interaction, we know that patient Ab are polyclonal and mostly target the N-terminal half of CASPR2 ectodomain (D-L1-L2-E1), all recognizing at least the discoidin and laminin G1 domains [6,11,12]. Moreover, patient Ab rarely target the C-terminal half of the protein (F-L3-E2-L4), where the main interaction domain of CASPR2, the laminin G4 domain, is located [11]. Thus, anti-CASPR2 autoAb would mainly perturb CASPR2/TAG-1 interaction trough the laminin G1 domain, which may explain their low propensity to impede CASPR2/TAG-1 interaction (Fig. 7B). In addition, in our cellular model, CASPR2/TAG-1 interactions are mainly occurring in cis with high constraints due to a complex environment, whereas in the solid phase binding assay, CASPR2 and TAG-1 can freely adopt several orientations. Such differences may

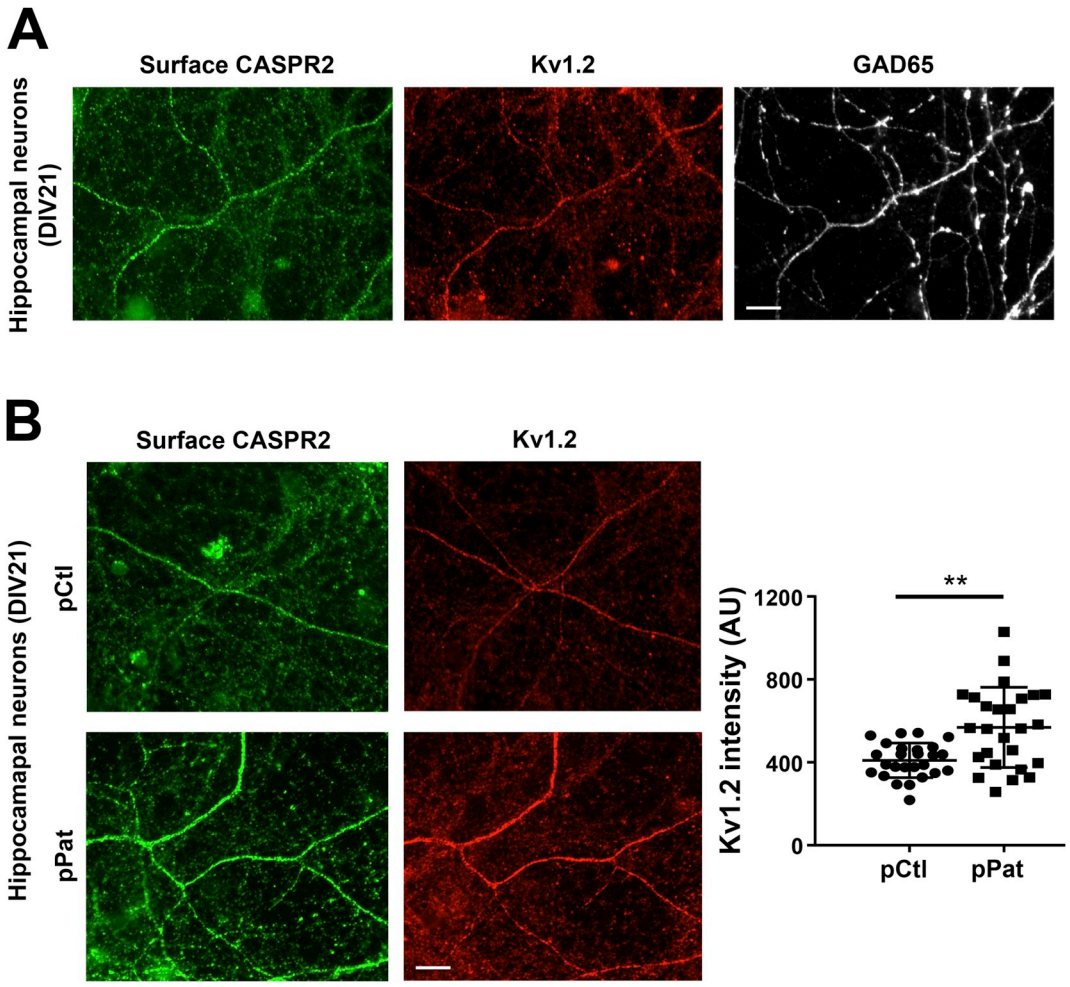

Fig. 6. Patient autoAb increase Kv1.2 expression in hippocampal neurons. A) hippocampal neurons (21 DIV) stained on live cells for surface Caspr2 and on permeabilized cells for Kv1.2 and GAD65. **B)** hippocampal neurons (21 DIV) treated for 24h with pooled patient (pPat) or control (pCtl) IgG were stained as in A) and Kv1.2 fluorescence signal intensities were quantified. n = 26 neurons per condition obtained from 3 independent experiments, **p < 0.01 Mann-Whitney test. Scale bar 10 μm.

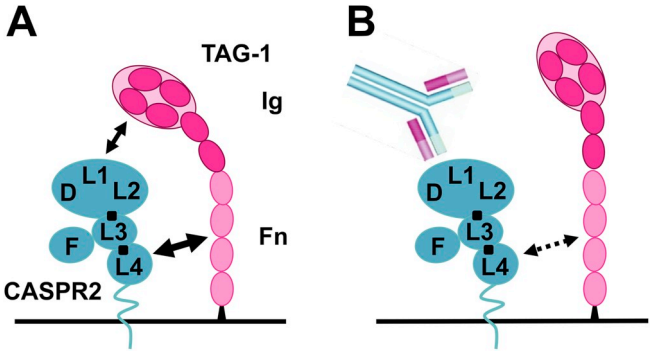

Fig. 7. Model of CASPR2/TAG-1 interaction and impact of anti-CASPR2 autoAb. A) Based on the molecular shape and dimension of these two molecules we propose a model for which laminin G4 (L4), the main interaction domain of CASPR2, interacts with the fibronectin (Fn) domains of TAG-1 and the laminin G1 (L1) domain of CASPR2 interacts with the immunoglobulin (Ig) domains of TAG-1. **B)** Since patient Ab rarely target the laminin G4 domain of the protein, anti-CASPR2 autoAb would mainly perturb CASPR2/TAG-1 interaction trough the laminin G1 domain.

explain the higher blocking propensity of patient Ab in the solid phase binding assay [20].

Besides, as for the solid phase binding assay, the extent of inhibition varied between patients although the 4 sera tested in this study presented similar anti-CASPR2 Ab titers. Differences in the localization of targeted epitopes or the Ab affinity/avidity for their targets as well as the Ab titer for each subclass of IgG (IgG1 or IgG4) may account for the variations in the degree of inhibition. Additional studies with higher number of patients are needed to determine factors responsible for the difference observed between patients.

4.3. CASPR2 and Kv1 expression are linked

We showed herein that the introduction of CASPR2 into HEK cells induces a marked increase of the level of Kv1.2 surface expression. Moreover, it appears that Caspr2-positive inhibitory neurons also express high level of Kv1.2. These results are in line with previous findings showing a decreased membrane expression of Kv1.2 in *Cntnap2* KO DRG neurons in culture. Notably, in these cells the KO of Caspr2 resulted in enhanced excitability with a large reduction in the DTX-sensitive outward current, indicating a reduction in the function of Kv1 channels [19]. Moreover, in wild-type DRG neurons cultured *in vitro* for 5 days, a spontaneous reduction in Kv1 (membrane) and Caspr2 (mRNA) expression coincided with hyperexcitabilty. Importantly, enhanced excitability was reversed by Caspr2-forced expression in a Kv1 channel-dependent manner [19]. Therefore, one can speculate that CASPR2, by interfering with surface expression of Kv1 channels is an important modulator of neuronal excitability.

4.4. Anti-CASPR2 patient autoAb increase Kv1.2 expression

In HEK cells, patient autoAb increase Kv1.2 surface expression. Importantly, such an increase is also observed in hippocampal neurons although we could not determine if this occurs at the cells surface. These results are in contrast with a previous study showing that in cultured DRG neurons treated with anti-CASPR2 patient Ab the number of cells expressing Kv1.2 at the surface was decreased [19]. Since Kv1 expression may vary with CASPR2 expression levels, it would be interesting to assess the impact of anti-CASPR2 autoAb on the level of CASPR2 surface expression in these neurons. Nevertheless, diverse mechanisms might regulate Kv1 surface expression depending on the cell type, in the same way as different mechanisms are responsible for Kv1 enrichment at the AIS and JXP. Of particular interest, a decrease of CASPR2 and Kv1.1 expression was observed at JXP following systemic injection of anti-CASPR2 patient Ab despite the fact that no patient Ab binding was detected in this region. On the other hand, a clear patient Ab binding was observed on DRG cell soma [19]. It is therefore tempting to speculate that decreased JXP expression of CASPR2 and Kv1.1 might be due to patient Ab-induced retention of these molecules at the soma, thereby impairing their axonal membrane lateral diffusion.

Since CASPR2 interacts with Kv1 channels indirectly through their intracellular cytoplasmic domains [1], the mechanism by which CASPR2 promotes Kv1.2 surface expression likely relies on intracellular motifs. Both proteins present a cytoskeleton-binding motif as well as a PDZ-binding motif, which could lead to restricted diffusion and co-clustering of CASPR2 and Kv1.2 at the membrane. For instance, the 4.1B-cytoskeleton-binding motif of CASPR2 was depicted as required for the enrichment of Kv1 channels at the NOR [35]. Kv1.2 surface expression relies on tyrosine residues present in its intracellular domain. Their phosphorylation leads to Kv1.2 reduced binding to the cytoskeleton and endocytosis [36,37]. Of particular interest, TAG-1-induced clustering of Kv1.2 along axons was shown to depend on Kv1.2 phosphorylation [29]. Whether CASPR2 could modulate Kv1 surface expression by impinging Kv1 phosphorylation directly or indirectly, by altering TAG-1 membrane distribution [15,29], remains to be established. Regarding the possible mechanism(s) by which anti-CASPR2 autoAb may lead to increased Kv1.2 expression, patient Ab binding may restrict CASPR2 diffusion thereby promoting cluster formation. This may in turn retain Kv1.2 at the membrane possibly by stabilizing CASPR2/Kv1.2 interactions, thus limiting Kv1 endocytosis.

Kv1 channels play a major role in membrane repolarization following action potential. A decrease in Kv1 expression leads to higher neuronal excitability characterized by an increase of action potential frequency and repolarization latency [38]. This results in increased neurotransmitter release at the synapse [39]. On the contrary, an increase of Kv1 expression could lead to a decrease of action potential frequency and neurotransmitter release [40]. Since CASPR2 is mainly expressed in inhibitory neurons, anti-CASPR2 autoAb, by increasing Kv1 expression, could specifically result in decreased inhibition, a defect consistent with the seizure disorders observed in patients.

In conclusion, we bring further evidences of two potential pathogenic mechanisms of anti-CASPR2 autoAb in patients with AE namely disturbing CASPR2/TAG-1 interaction and Kv1.2 expression. By impacting on neuronal excitability, these pathogenic mechanisms could contribute to the clinical features of patients with AE. Furthermore, our data provide new insights into the interaction constraints between CASPR2 and TAG-1, which might prove useful to study the relevance of this interaction in the formation and localization of the CASPR2/TAG-1/Kv1 complex.

Funding

This work was supported by INSERM, CNRS, University Lyon 1, the Agence Nationale de la Recherche (ANR-14-CE15-0001-MECANO), France, the Fondation pour la Recherche Médicale (FRM DQ20170336751), France and the fonds de dotation CSL Behring pour la recherche, France.

Acknowledgements

We are grateful to C. Faivre-Sarrailh (Institut de Neurobiologie de la Méditerranée, Aix Marseille Université, INSERM UMR1249, Marseille France) for providing the CASPR2 full-length and derived plasmids as well as scientific and technical advice. We thank Anthony Morielli (University of Vermont, Burlington USA) for providing the HEK-Kv cell line and, A. Vandermoeten, LM. Illartein, O. Martin and A. Meunier (Scar, Faculté Rockefeller, Lyon) for taking care of the animals.

Appendix A. Supplementary data

Supplementary data to this article can be found online at https://doi.org/10.1016/j.jaut.2019.05.012.

References

[1] S. Poliak, L. Gollan, R. Martinez, A. Custer, S. Einheber, J.L. Salzer, J.S. Trimmer, P. Shrager, E. Peles, Caspr2, a new member of the neurexin superfamily, is localized at the juxtaparanodes of myelinated axons and associates with K+ channels, Neuron 24 (1999) 1037–1047.

[2] P. Shillito, P.C. Molenaar, A. Vincent, K. Leys, W. Zheng, R.J. van den Berg, J.J. Plomp, G.T. van Kempen, G. Chauplannaz, A.R. Wintzen, Acquired neuromyotonia: evidence for autoantibodies directed against K+ channels of peripheral nerves, Ann. Neurol. 38 (1995) 714–722, https://doi.org/10.1002/ana.410380505.

[3] R. Liguori, A. Vincent, L. Clover, P. Avoni, G. Plazzi, P. Cortelli, A. Baruzzi, T. Carey, P. Gambetti, E. Lugaresi, P. Montagna, Morvan's syndrome: peripheral and central nervous system and cardiac involvement with antibodies to voltage-gated potassium channels, Brain J. Neurol. 124 (2001) 2417–2426.

[4] C. Buckley, J. Oger, L. Clover, E. Tüzün, K. Carpenter, M. Jackson, A. Vincent, Potassium channel antibodies in two patients with reversible limbic encephalitis, Ann. Neurol. 50 (2001) 73–78.

[5] J. Newsom-Davis, C. Buckley, L. Clover, I. Hart, P. Maddison, E. Tüzüm, A. Vincent, Autoimmune disorders of neuronal potassium channels, Ann. N. Y. Acad. Sci. 998 (2003) 202–210.

[6] B. Joubert, M. Saint-Martin, N. Noraz, G. Picard, V. Rogemond, F. Ducray, V. Desestret, D. Psimaras, J.-Y. Delattre, J.-C. Antoine, J. Honnorat, Characterization of a subtype of autoimmune encephalitis with anti-contactin-associated protein-like 2 antibodies in the cerebrospinal fluid, prominent limbic symptoms, and seizures, JAMA Neurol 73 (2016) 1115–1124, https://doi.org/10.1001/jamaneurol.2016.1585.

[7] A. van Sonderen, H. Ariño, M. Petit-Pedrol, F. Leypoldt, P. Körtvélyessy, K.-P. Wandinger, E. Lancaster, P.W. Wirtz, M.W.J. Schreurs, P.A.E. Sillevis Smitt, F. Graus, J. Dalmau, M.J. Titulaer, The clinical spectrum of Caspr2 antibody-associated disease, Neurology 87 (2016) 521–528, https://doi.org/10.1212/WNL.0000000000002917.

[8] S.R. Irani, S. Alexander, P. Waters, K.A. Kleopa, P. Pettingill, L. Zuliani, E. Peles, C. Buckley, B. Lang, A. Vincent, Antibodies to Kv1 potassium channel-complex proteins leucine-rich, glioma inactivated 1 protein and contactin-associated protein-2 in limbic encephalitis, Morvan's syndrome and acquired neuromyotonia, Brain 133 (2010) 2734–2748, https://doi.org/10.1093/brain/awq213.

[9] M. Lai, M.G.M. Huijbers, E. Lancaster, F. Graus, L. Bataller, R. Balice-Gordon, J.K. Cowell, J. Dalmau, Investigation of LGI1 as the antigen in limbic encephalitis previously attributed to potassium channels: a case series, Lancet Neurol. 9 (2010) 776–785, https://doi.org/10.1016/S1474-4422(10)70137-X.

[10] M. Saint-Martin, B. Joubert, V. Pellier-Monnin, O. Pascual, N. Noraz, J. Honnorat, Contactin-associated protein-like 2, a protein of the neurexin family involved in several human diseases, Eur. J. Neurosci. 48 (2018) 1906–1923, https://doi.org/10.1111/ejn.14081.

[11] A.L. Olsen, Y. Lai, J. Dalmau, S.S. Scherer, E. Lancaster, Caspr2 autoantibodies target multiple epitopes, Neurol. Neuroimmunol. Neuroinflammation. 2 (2015) e127, https://doi.org/10.1212/NXI.0000000000000127.

[12] D. Pinatel, B. Hivert, J. Boucraut, M. Saint-Martin, V. Rogemond, L. Zoupi, D. Karagogeos, J. Honnorat, C. Faivre-Sarrailh, Inhibitory axons are targeted in hippocampal cell culture by anti-Caspr2 autoantibodies associated with limbic encephalitis, Front. Cell. Neurosci. 9 (2015) 265, https://doi.org/10.3389/fncel.2015.00265.

[13] S. Poliak, D. Salomon, H. Elhanany, H. Sabanay, B. Kiernan, L. Pevny, C.L. Stewart, X. Xu, S.-Y. Chiu, P. Shrager, A.J.W. Furley, E. Peles, Juxtaparanodal clustering of Shaker-like K+ channels in myelinated axons depends on Caspr2 and TAG-1, J. Cell Biol. 162 (2003) 1149–1160, https://doi.org/10.1083/jcb.200305018.

[14] M.N. Rasband, E.W. Park, D. Zhen, M.I. Arbuckle, S. Poliak, E. Peles, S.G.N. Grant, J.S. Trimmer, Clustering of neuronal potassium channels is independent of their interaction with PSD-95, J. Cell Biol. 159 (2002) 663–672, https://doi.org/10.1083/jcb.200206024.

[15] M. Traka, L. Goutebroze, N. Denisenko, M. Bessa, A. Nifli, S. Havaki, Y. Iwakura, F. Fukamauchi, K. Watanabe, B. Soliven, J.-A. Girault, D. Karagogeos, Association of

TAG-1 with Caspr2 is essential for the molecular organization of juxtaparanodal regions of myelinated fibers, J. Cell Biol. 162 (2003) 1161–1172, https://doi.org/10.1083/jcb.200305078.
[16] N. Chen, F. Koopmans, A. Gordon, I. Paliukhovich, R.V. Klaassen, R.C. van der Schors, E. Peles, M. Verhage, A.B. Smit, K.W. Li, Interaction proteomics of canonical Caspr2 (CNTNAP2) reveals the presence of two Caspr2 isoforms with overlapping interactomes, Biochim. Biophys. Acta 1854 (2015) 827–833, https://doi.org/10.1016/j.bbapap.2015.02.008.
[17] M.C. Inda, J. DeFelipe, A. Muñoz, Voltage-gated ion channels in the axon initial segment of human cortical pyramidal cells and their relationship with chandelier cells, Proc. Natl. Acad. Sci. U.S.A. 103 (2006) 2920–2925, https://doi.org/10.1073/pnas.0511197103.
[18] R. Scott, A. Sánchez-Aguilera, K. van Elst, L. Lim, N. Dehorter, S.E. Bae, G. Bartolini, E. Peles, M.J.H. Kas, H. Bruining, O. Marín, Loss of Cntnap2 causes axonal excitability deficits, developmental delay in cortical myelination, and abnormal stereotyped motor behavior, Cereb. Cortex N. Y. N 29 (2019) 586–597, https://doi.org/10.1093/cercor/bhx341 1991.
[19] J.M. Dawes, G.A. Weir, S.J. Middleton, R. Patel, K.I. Chisholm, P. Pettingill, L.J. Peck, J. Sheridan, A. Shakir, L. Jacobson, M. Gutierrez-Mecinas, J. Galino, J. Walcher, J. Kühnemund, H. Kuehn, M.D. Sanna, B. Lang, A.J. Clark, A.C. Themistocleous, N. Iwagaki, S.J. West, K. Werynska, L. Carroll, T. Trendafilova, D.A. Menassa, M.P. Giannoccaro, E. Coutinho, I. Cervellini, D. Tewari, C. Buckley, M.I. Leite, H. Wildner, H.U. Zeilhofer, E. Peles, A.J. Todd, S.B. McMahon, A.H. Dickenson, G.R. Lewin, A. Vincent, D.L. Bennett, Immune or genetic-mediated disruption of CASPR2 causes pain hypersensitivity due to enhanced primary afferent excitability, Neuron 97 (2018) 806–822, https://doi.org/10.1016/j.neuron.2018.01.033 e10.
[20] K.R. Patterson, J. Dalmau, E. Lancaster, Mechanisms of Caspr2 antibodies in autoimmune encephalitis and neuromyotonia, Ann. Neurol. 83 (2018) 40–51, https://doi.org/10.1002/ana.25120.
[21] B. Joubert, F. Gobert, L. Thomas, M. Saint-Martin, V. Desestret, P. Convers, V. Rogemond, G. Picard, F. Ducray, D. Psimaras, J.-C. Antoine, J.-Y. Delattre, J. Honnorat, Autoimmune episodic ataxia in patients with anti-CASPR2 antibody-associated encephalitis, Neurol. Neuroimmunol. Neuroinflammation. 4 (2017) e371, https://doi.org/10.1212/NXI.0000000000000371.
[22] A. Tzimourakas, S. Giasemi, M. Mouratidou, D. Karagogeos, Structure-function analysis of protein complexes involved in the molecular architecture of juxtaparanodal regions of myelinated fibers, Biotechnol. J. 2 (2007) 577–583, https://doi.org/10.1002/biot.200700023.
[23] T.G. Cachero, A.D. Morielli, E.G. Peralta, The small GTP-binding protein RhoA regulates a delayed rectifier potassium channel, Cell 93 (1998) 1077–1085.
[24] E. Nesti, B. Everill, A.D. Morielli, Endocytosis as a mechanism for tyrosine kinase-dependent suppression of a voltage-gated potassium channel, Mol. Biol. Cell 15 (2004) 4073–4088, https://doi.org/10.1091/mbc.e03-11-0788.
[25] M. Savvaki, K. Theodorakis, L. Zoupi, A. Stamatakis, S. Tivodar, K. Kyriacou, F. Stylianopoulou, D. Karagogeos, The expression of TAG-1 in glial cells is sufficient for the formation of the juxtaparanodal complex and the phenotypic rescue of tag-1 homozygous mutants in the CNS, J. Neurosci. 30 (2010) 13943–13954, https://doi.org/10.1523/JNEUROSCI.2574-10.2010.
[26] D. Pinatel, B. Hivert, M. Saint-Martin, N. Noraz, M. Savvaki, D. Karagogeos, C. Faivre-Sarrailh, The Kv1-associated molecules TAG-1 and Caspr2 are selectively targeted to the axon initial segment in hippocampal neurons, J. Cell Sci. 130 (2017) 2209–2220, https://doi.org/10.1242/jcs.202267.
[27] C. Rader, B. Kunz, R. Lierheimer, R.J. Giger, P. Berger, P. Tittmann, H. Gross, P. Sonderegger, Implications for the domain arrangement of axonin-1 derived from the mapping of its NgCAM binding site, EMBO J. 15 (1996) 2056–2068.
[28] B. Kunz, R. Lierheimer, C. Rader, M. Spirig, U. Ziegler, P. Sonderegger, Axonin-1/TAG-1 mediates cell-cell adhesion by a cis-assisted trans-interaction, J. Biol. Chem. 277 (2002) 4551–4557, https://doi.org/10.1074/jbc.M109779200.
[29] C. Gu, Y. Gu, Clustering and activity tuning of Kv1 channels in myelinated hippocampal axons, J. Biol. Chem. 286 (2011) 25835–25847, https://doi.org/10.1074/jbc.M111.219113.
[30] M.G. Huijbers, L.A. Querol, E.H. Niks, J.J. Plomp, S.M. van der Maarel, F. Graus, J. Dalmau, I. Illa, J.J. Verschuuren, The expanding field of IgG4-mediated neurological autoimmune disorders, Eur. J. Neurol. 22 (2015) 1151–1161, https://doi.org/10.1111/ene.12758.
[31] E.N. Rubio-Marrero, G. Vincelli, C.M. Jeffries, T.R. Shaikh, I.S. Pakos, F.M. Ranaivoson, S. von Daake, B. Demeler, A. De Jaco, G. Perkins, M.H. Ellisman, J. Trewhella, D. Comoletti, Structural characterization of the extracellular domain of CASPR2 and insights into its association with the novel ligand Contactin1, J. Biol. Chem. 291 (2016) 5788–5802, https://doi.org/10.1074/jbc.M115.705681.
[32] Z. Lu, M.V.V.V.S. Reddy, J. Liu, A. Kalichava, J. Liu, L. Zhang, F. Chen, Y. Wang, L.M.F. Holthauzen, M.A. White, S. Seshadrinathan, X. Zhong, G. Ren, G. Rudenko, Molecular architecture of contactin-associated protein-like 2 (CNTNAP2) and its interaction with contactin 2 (CNTN2), J. Biol. Chem. (2016), https://doi.org/10.1074/jbc.M116.748236 jbc.M116.748236.
[33] F. Chen, V. Venugopal, B. Murray, G. Rudenko, The structure of neurexin 1α reveals features promoting a role as synaptic organizer, Struct. Lond. Engl. 19 (2011) 779–789, https://doi.org/10.1016/j.str.2011.03.012 1993.
[34] C. Reissner, F. Runkel, M. Missler, Neurexins, Genome Biol. 14 (2013) 213, https://doi.org/10.1186/gb-2013-14-9-213.
[35] I. Horresh, V. Bar, J.L. Kissil, E. Peles, Organization of myelinated axons by Caspr and Caspr2 requires the cytoskeletal adapter protein 4.1B, J. Neurosci. Off. J. Soc. Neurosci. 30 (2010) 2480–2489, https://doi.org/10.1523/JNEUROSCI.5225-09.2010.
[36] D. Hattan, E. Nesti, T.G. Cachero, A.D. Morielli, Tyrosine phosphorylation of Kv1.2 modulates its interaction with the actin-binding protein cortactin, J. Biol. Chem. 277 (2002) 38596–38606, https://doi.org/10.1074/jbc.M205005200.
[37] H.C. Lai, L.Y. Jan, The distribution and targeting of neuronal voltage-gated ion channels, Nat. Rev. Neurosci. 7 (2006) 548–562, https://doi.org/10.1038/nrn1938.
[38] S.L. Smart, V. Lopantsev, C.L. Zhang, C.A. Robbins, H. Wang, S.Y. Chiu, P.A. Schwartzkroin, A. Messing, B.L. Tempel, Deletion of the K(V)1.1 potassium channel causes epilepsy in mice, Neuron 20 (1998) 809–819.
[39] J.R. Geiger, P. Jonas, Dynamic control of presynaptic Ca(2+) inflow by fast-inactivating K(+) channels in hippocampal mossy fiber boutons, Neuron 28 (2000) 927–939.
[40] S. He, L.-R. Shao, W.B. Rittase, S.B. Bausch, Increased Kv1 channel expression may contribute to decreased sIPSC frequency following chronic inhibition of NR2B-containing NMDAR, Neuropsychopharmacology 37 (2012) 1338–1356, https://doi.org/10.1038/npp.2011.320.